Supplementary materials

Effects of intra-seasonal drought on kinetics of tracheid differentiation and seasonal growth dynamics of Norway spruce along an elevational gradient

Dominik Florian Stangler [1]*, Hans-Peter Kahle [1], Martin Raden [1,2], Elena Larysch [1], Thomas Seifert [1,3] and Heinrich Spiecker [1]

[1] Chair of Forest Growth and Dendroecology, Albert-Ludwigs-University Freiburg, Tennenbacher Str. 4, 79106 Freiburg, Germany; Hans-Peter.Kahle@iww.uni-freiburg.de (H.-P.K.); Elena.Larysch@iww.uni-freiburg.de (E.L.); instww@uni-freiburg.de (H.S.)

[2] Bioinformatics Group, Department of Computer Science, Albert-Ludwigs-University Freiburg, Georges-Köhler-Allee 106, 79110 Freiburg, Germany; mmann@informatik.uni-freiburg.de (M.R.)

[3] Department of Forest and Wood Science, Stellenbosch University, Private Bag X1, 7602 Matieland, South Africa; Thomas.Seifert@iww.uni-freiburg.de (T.S.)

* Correspondence: Dominik.Stangler@iww.uni-freiburg.de (D.F.S.); Tel.: +49-761-203-8543

Modeling the seasonal variation of cell numbers in each developmental phase

The raw count data of the enlarging, wall thickening and mature phases were first normalized on the individual tree-level to account for unequal growth rates along the stem circumference following the approach by Rossi et al. [1]. Raw data of cambial cells were not normalized as it occasionally led to unrealistic numbers of cells in the dormancy phase presenting values actually never existing in nature. Furthermore, the number of cambial cells were not included in the modeling steps described below and only used for descriptive statistics within this study.

The process of cambial xylem cell production can be considered completed if no more enlarging cells are visible within a sample [2]. Therefore, the normalized data was further harmonized in order to ease the modeling procedure by replacing for each tree j within site i all weekly counted total xylem cell numbers after the cessation of cell enlargement ($cE_{i,j}$) until the last sampling date with the average value of weekly counted total cell numbers of all samples from the same time period ($nT_{i,j}$). By this data harmonization before model fitting, the transformed data kept the total numbers of produced tracheids after the end of cell enlargement in late summer/early autumn constant. In case, the weekly total cell numbers before the end of cell enlargement reached already higher values than $nT_{i,j}$, the values were harmonized accordingly.

To gain biologically meaningful results, when modeling the duration of tracheid differentiation of conifers in temperate climates, three important preconditions must be fulfilled. First, the models predicting for each day of year t the number of the mature cells ($nM_{i,j,t}$), as well as the number of cells with secondary cell walls ($nWM_{i,j,t}$) and the total number of xylem cells ($nEWM_{i,j,t}$) must be monotonically increasing functions. Second, with exception of the asymptotes or during intra-seasonal dormancy periods, the three functions are not supposed to intersect at any point of time during the growing season. And third, they must converge at the same upper asymptote (i.e. $nT_{i,j}$). after the cessation of cell enlargement $cE_{i,j}$ for $nWM_{i,j,t}$ and $nEWM_{i,j,t}$ and after the cessation of cell wall thickening $cW_{i,j}$ for $nM_{i,j,t}$. In the following, we provide a detailed description, how we modeled

the seasonal variation of cell numbers in each developmental phase and how we derived the three functions of $nM_{i,j,t}$, $nWM_{i,j,t}$ and $nEWM_{i,j,t}$ fulfilling the above-mentioned preconditions.

To predict for each day of year t, for each elevation site i and the individual tree j the number of cambial cells ($nC_{i,j,t}$), we fitted generalized additive mixed models (GAMMs) with day of year as fixed effect and individual tree as random effect to the weekly raw data of the number of cambial cells $nC_{i,j,t}^{raw}$ [3]. The choice of the best basis dimension (k-value) defining the smoothness of the model was based on minimizing the AIC value. All GAMMs were specified in the *mgcv* package of the R-environment using log as a link function and Poisson as error distribution.

GAMMs (denotated as ^{G}) were fitted to the harmonized weekly counts of enlargement cells $nE_{j,i,t}^{harm}$ and secondary wall thickening cells $nW_{j,i,t}^{harm}$ to predict for each day of year the number of cells in the corresponding cell differentiation phases $nE_{j,i,t}^{G}$ and $nW_{j,i,t}^{G}$. Analogously, we fitted shape constrained additive mixed models (SCAMMs, denotated as ^{S}) to the harmonized weekly numbers of mature cells $nM_{j,i,t}^{harm}$ and total number of xylem cells $nEWM_{j,i,t}^{harm}$ using the *scam* package to predict for each day of year the number of cells in the corresponding functions $nM_{j,i,t}^{S}$ and $nEWM_{j,i,t}^{S}$ [4]. SCAMMs were specified with monotonically increasing shape constraints while using "nlm" as numerical optimization method, log as a link function and Poisson as an error distribution. In order to optimize the fitting to the lower and upper asymptotes of $nEWM_{j,i,t}^{harm}$, all observations before the beginning of cell enlargement ($bE_{i,j}$) and after the cessation of cell enlargement ($cE_{i,j}$) were weighted by a factor of 10000 during the fitting procedure. The fitting of the lower and upper asymptotes of $nM_{j,i,t}^{harm}$ was done accordingly, however weighting all observations before the beginning of cell maturity ($bM_{j,i}$) and after cessation of secondary wall thickening ($cW_{j,i}$) with the same factor.

To ensure coherence of the modeling framework (i.e. that the equations $nWM_{i,j,t} = nW_{i,j,t} + nM_{i,j,t}$ and $nEWM_{i,j,t} = nE_{i,j,t} + nW_{i,j,t} + nM_{i,j,t}$ are generally valid), the predictions of the GAMMs and SCAMMs were integrated in the following equations to predict for each day of year t the definite number of cells in cell enlargement ($nE_{i,j,t}$), number of cells in secondary wall thickening ($nW_{i,j,t}$), the number of mature cells ($nM_{i,j,t}$), the number of cells with secondary walls ($nWM_{i,j,t}$) and the total number of xylem cells ($nEWM_{i,j,t}$):

$$nEWM_{i,j,t} = nEWM_{i,j,t}^{S} \tag{S1}$$

$$nE_{i,j,t} = \frac{nE_{i,j,t}^{G}}{nE_{i,j,t}^{G} + nW_{i,j,t}^{G} + nM_{i,j,t}^{S}} \times nEWM_{i,j,t} \tag{S2}$$

$$nW_{i,j,t} = \frac{nW_{i,j,t}^{G}}{nE_{i,j,t}^{G} + nW_{i,j,t}^{G} + nM_{i,j,t}^{S}} \times nEWM_{i,j,t} \tag{S3}$$

$$nM_{i,j,t} = \frac{nM_{i,j,t}^{S}}{nE_{i,j,t}^{G} + nW_{i,j,t}^{G} + nM_{i,j,t}^{S}} \times nEWM_{i,j,t} \tag{S4}$$

$$nWM_{i,j,t} = nW_{i,j,t} + nM_{i,j,t} \tag{S5}$$

where we simulated all possible combinations of basis dimensions between 5 to 15 for all models and ranked the constellations based on minimizing for each combination the arithmetic mean of the

ΔAICs calculated as the difference of the AIC of the individual models and the corresponding best model with the lowest AIC value. Combinations of base dimensions were excluded from the model selection, in case one of the abovementioned three important preconditions of the modeling framework were violated.
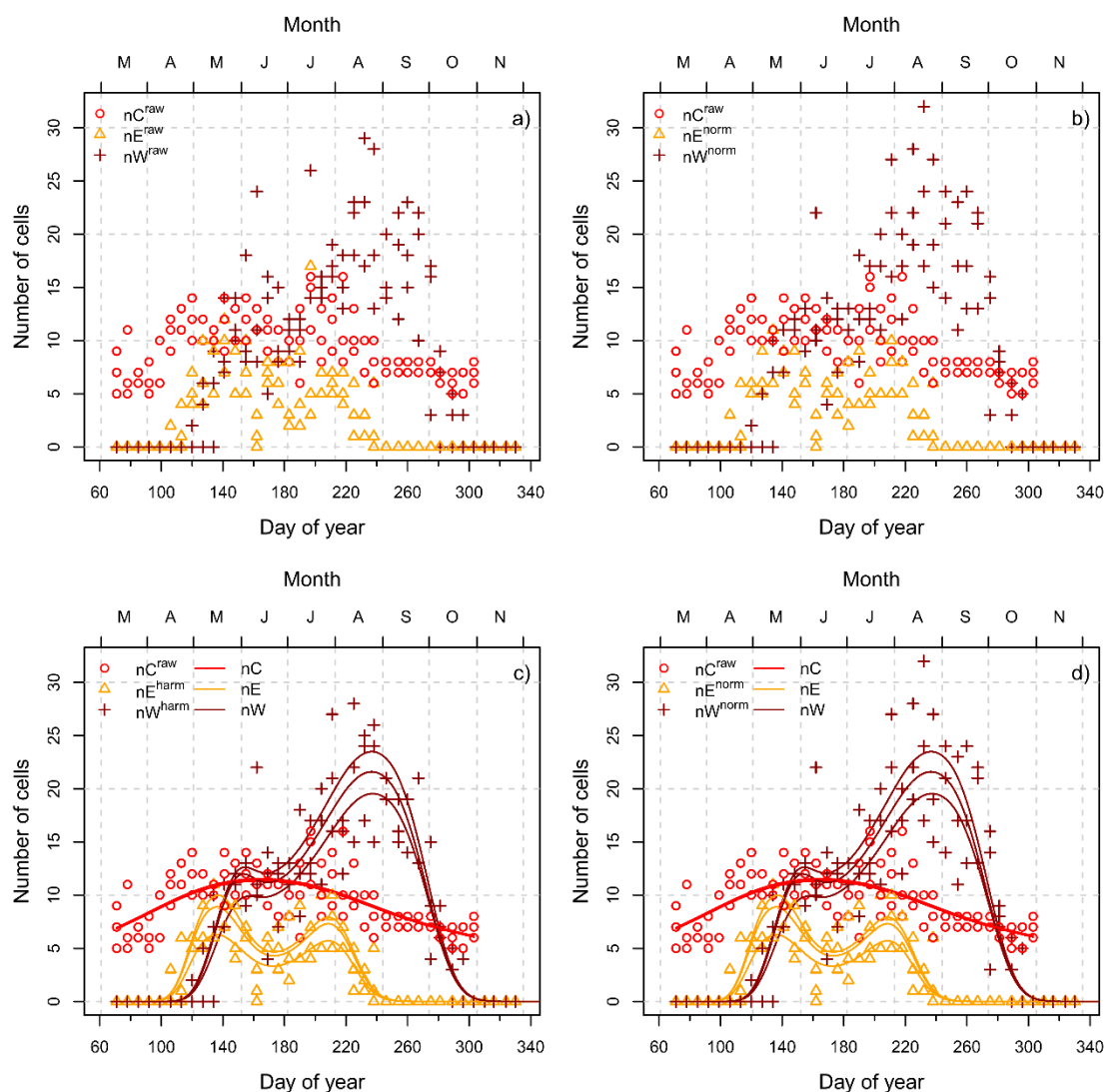
450 m a.s.l

Figure S1. 450 m a.s.l. elevation site: (**a**) Raw data of weekly counts of cambial cells (nC^{raw}), enlarging cells (nE^{raw}) and wall thickening cells (nW^{raw}), (**b**) Raw data of cambial cells (nC^{raw}), as well as normalized data of enlarging cells (nE^{norm}) and wall thickening cells (nW^{norm}), **(c-d)** Tree individual predictions of the definite daily number of cambial cells (nC), enlarging cells (nE) and wall thickening cells (nW) based on generalized additive mixed models in comparison to the raw (nC^{raw}), harmonized (nE^{harm}, nW^{harm}) and normalized data (nE^{norm}, nW^{norm}). One data point reflects for each day of year one of three sampled trees
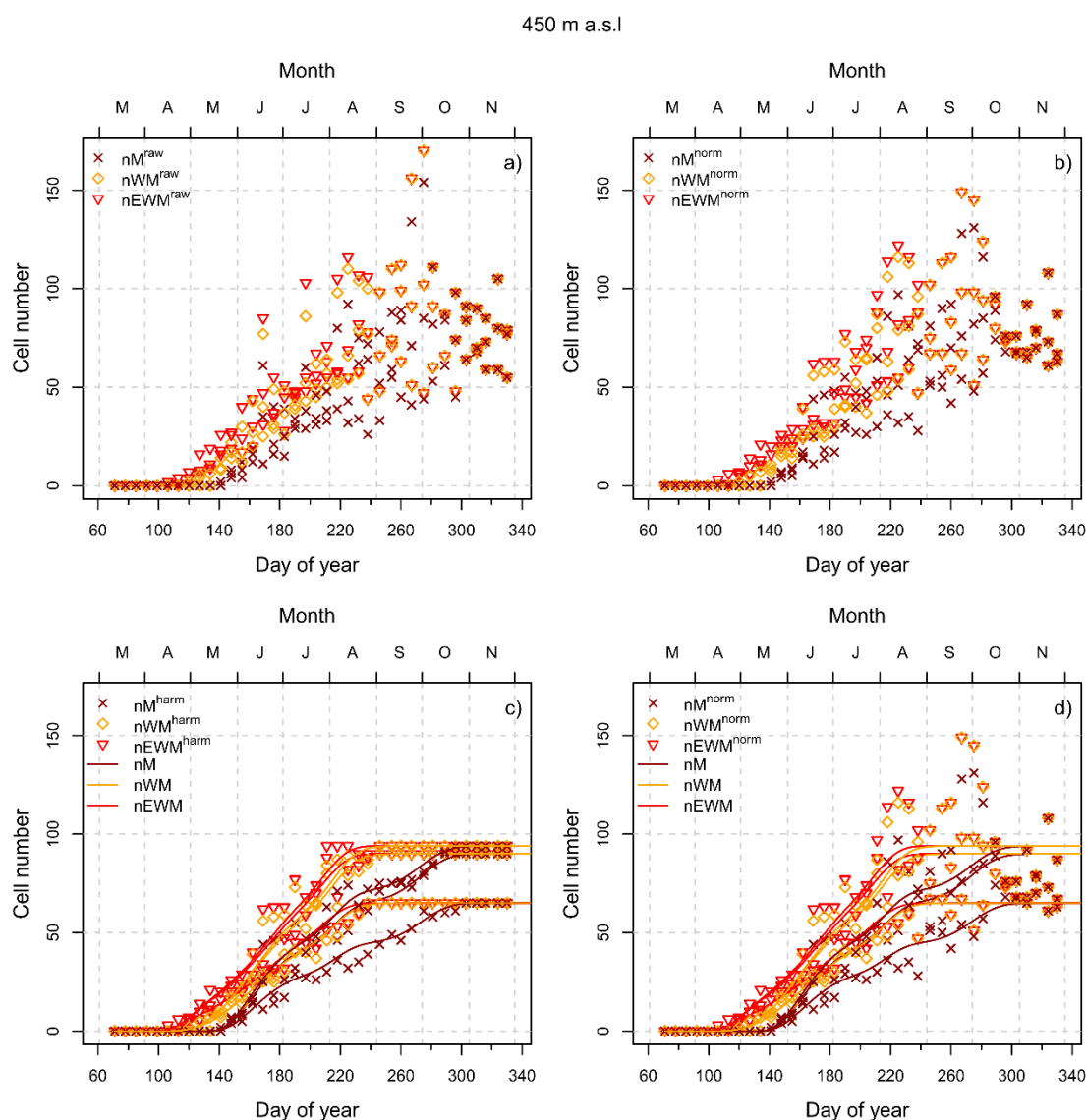
450 m a.s.l

Figure S2. 450 m a.s.l. elevation site: (**a**) Raw data of weekly counts of mature cells (*nM^raw^*), cells with secondary cell walls (*nWM^raw^*) and total number of xylem cells (*nEWM^raw^*), (**b**) Normalized data of mature cells (*nM^norm^*), cells with secondary cell walls (*nWM^norm^*) and total number of xylem cells (*nEWM^norm^*), (**c-d**) Tree individual predictions of the definite daily number of mature cells (*nM*), cells with secondary walls (*nWM*) and total number of xylem cells (*nEWM*) based on shape constrained additive mixed models in comparison to the harmonized (*nM ^harm^*, *nWM ^harm^*, *nEWM ^harm^*) and normalized data (*nM ^norm^*, *nWM ^norm^*, *nEWM ^norm^*). One data point reflects for each day of year one of three sampled trees.
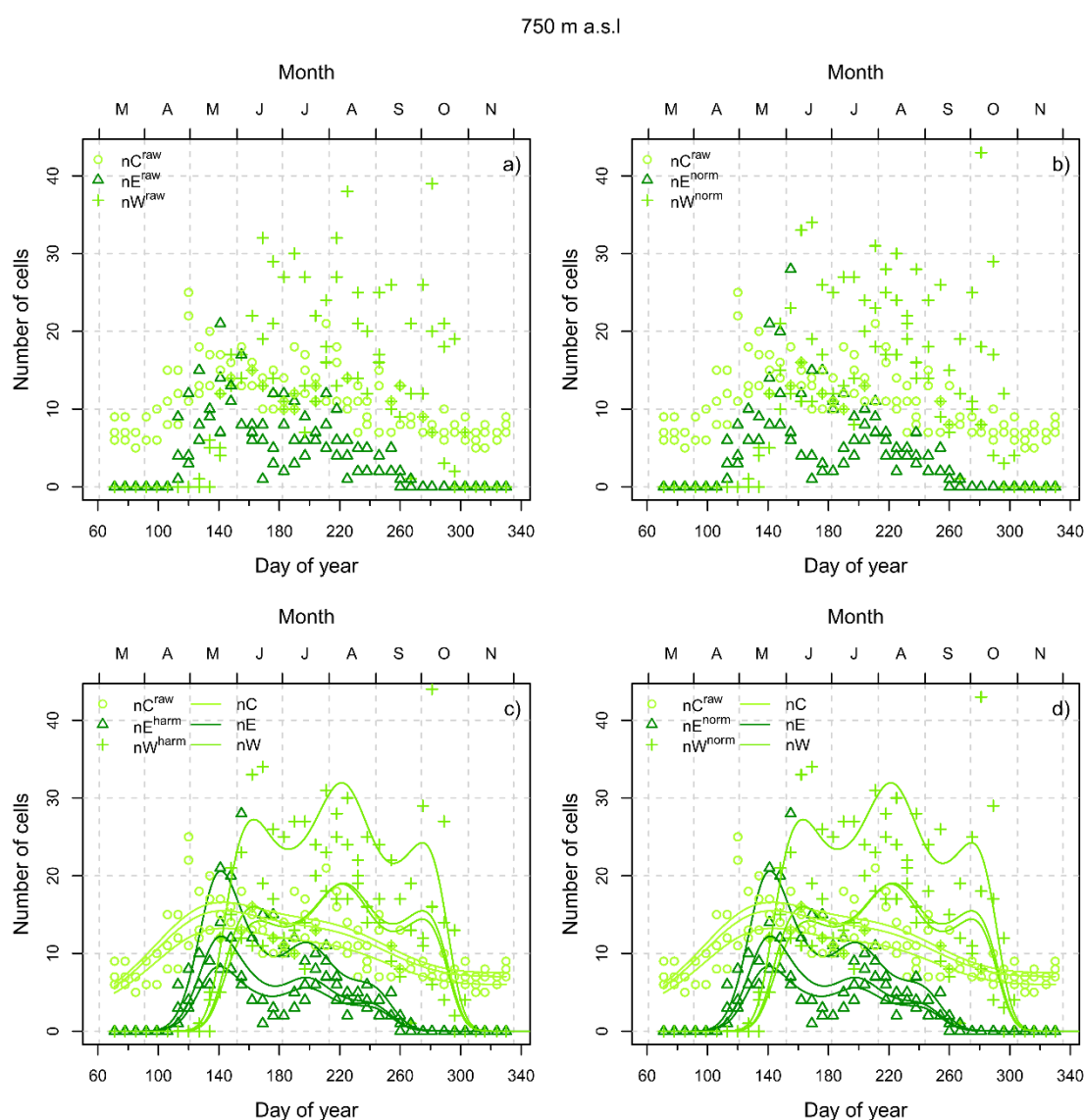
Figure S3. 750 m a.s.l. elevation site: (**a**) Raw data of weekly counts of cambial cells (nC^{raw}), enlarging cells (nE^{raw}) and wall thickening cells (nW^{raw}), (**b**) Raw data of cambial cells (nC^{raw}), as well as normalized data of enlarging cells (nE^{norm}) and wall thickening cells (nW^{norm}), (**c-d**) Tree individual predictions of the definite daily number of cambial cells (nC), enlarging cells (nE) and wall thickening cells (nW) based on generalized additive mixed models in comparison to the raw (nC^{raw}), harmonized (nE^{harm}, nW^{harm}) and normalized data (nE^{norm}, nW^{norm}). One data point reflects for each day of year one of three sampled trees
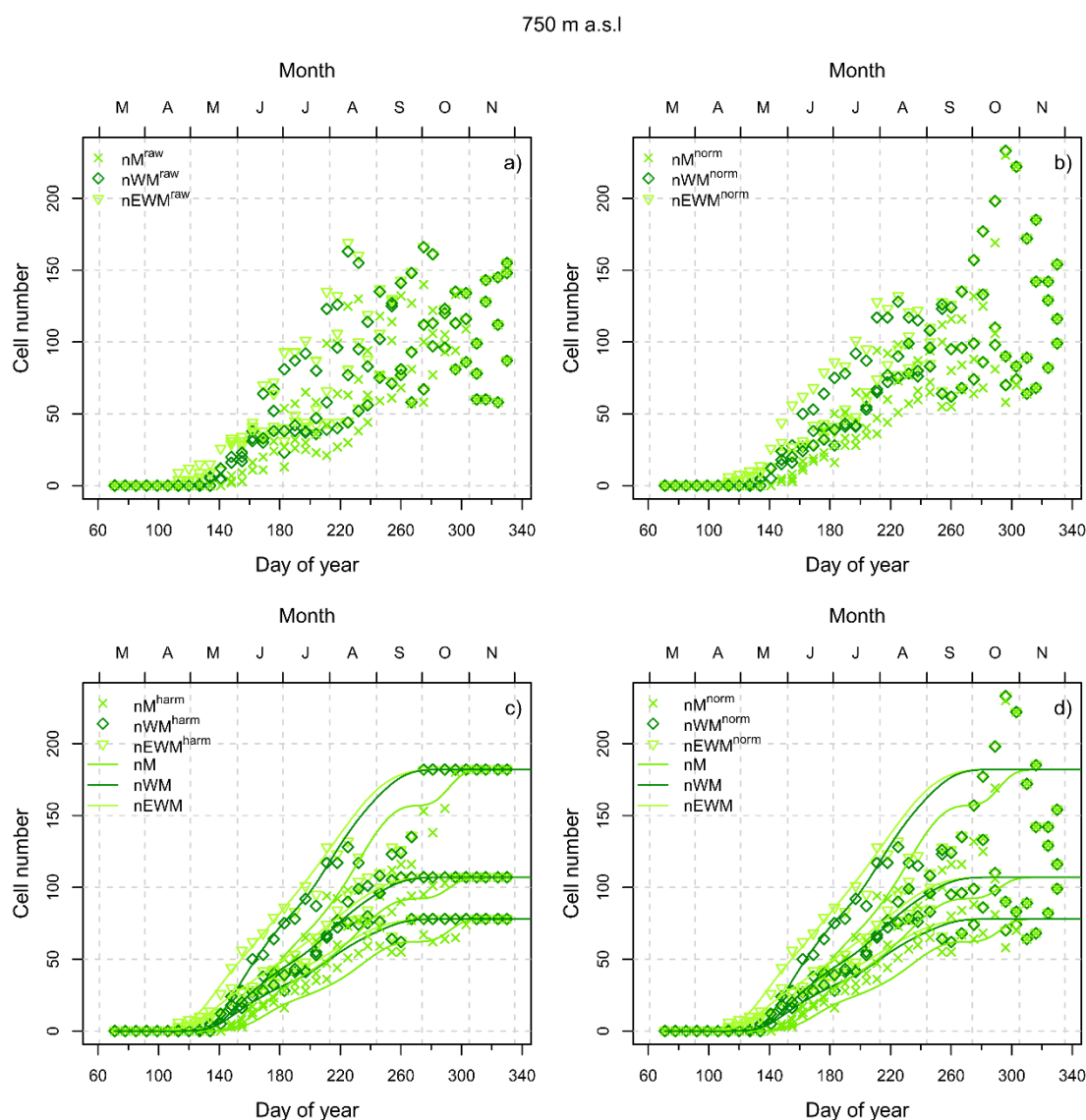
Figure S4. 750 m a.s.l. elevation site: (**a**) Raw data of weekly counts of mature cells (nM^{raw}), cells with secondary cell walls (nWM^{raw}) and total number of xylem cells ($nEWM^{raw}$), (**b**) Normalized data of mature cells (nM^{norm}), cells with secondary cell walls (nWM^{norm}) and total number of xylem cells ($nEWM^{norm}$), (**c-d**) Tree individual predictions of the definite daily number of mature cells (nM), cells with secondary walls (nWM) and total number of xylem cells ($nEWM$) based on shape constrained additive mixed models in comparison to the harmonized (nM^{harm}, nWM^{harm}, $nEWM^{harm}$) and normalized data (nM^{norm}, nWM^{norm}, $nEWM^{norm}$). One data point reflects for each day of year one of three sampled trees.
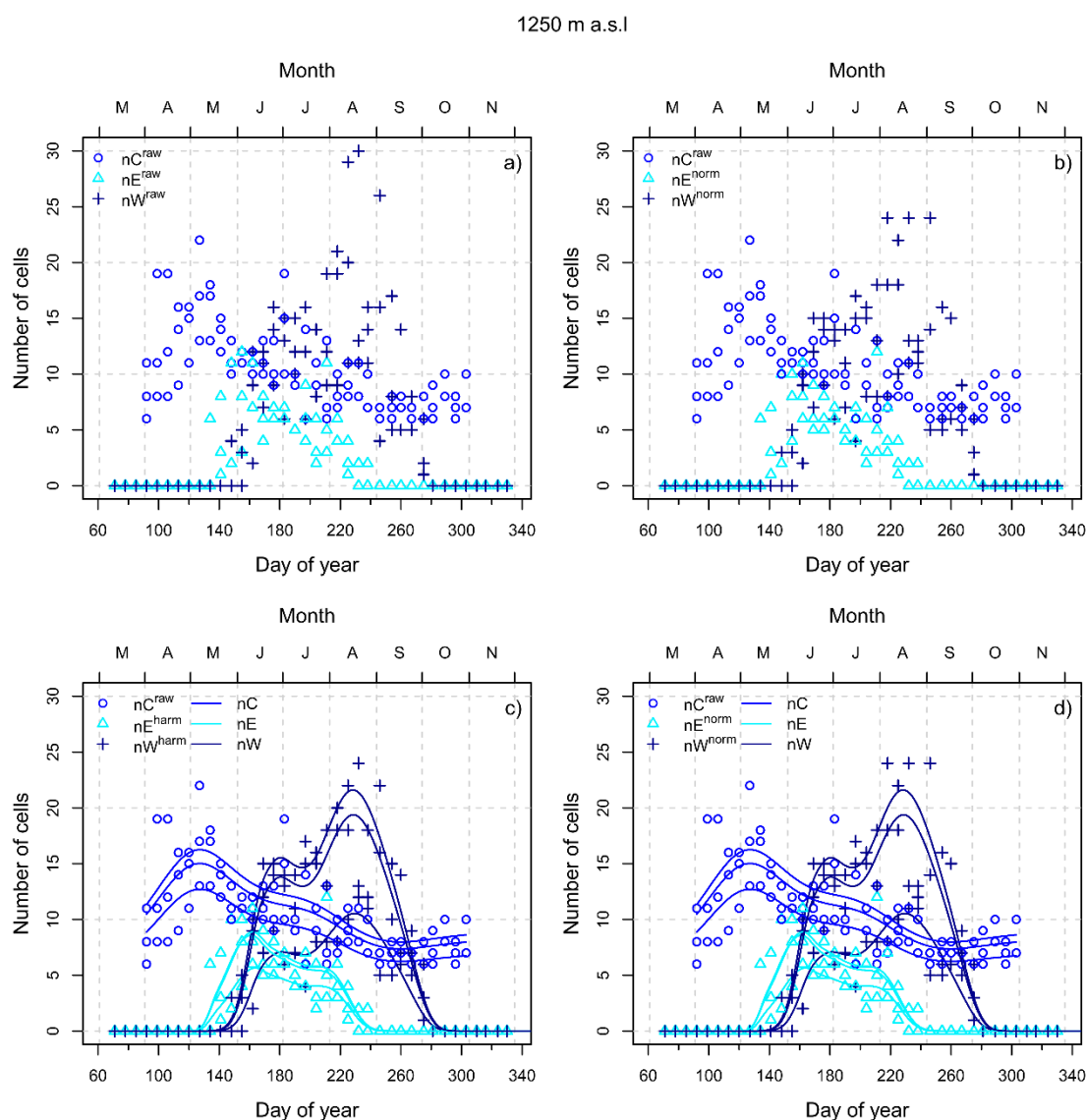
Figure S5. 1250 m a.s.l. elevation site: (**a**) Raw data of weekly counts of cambial cells (nC^{raw}), enlarging cells (nE^{raw}) and wall thickening cells (nW^{raw}), (**b**) Raw data of cambial cells (nC^{raw}), as well as normalized data of enlarging cells (nE^{norm}) and wall thickening cells (nW^{norm}), **(c-d)** Tree individual predictions of the definite daily number of cambial cells (nC), enlarging cells (nE) and wall thickening cells (nW) based on generalized additive mixed models in comparison to the raw (nC^{raw}), harmonized (nE^{harm}, nW^{harm}) and normalized data (nE^{norm}, nW^{norm}). One data point reflects for each day of year one of three sampled trees.
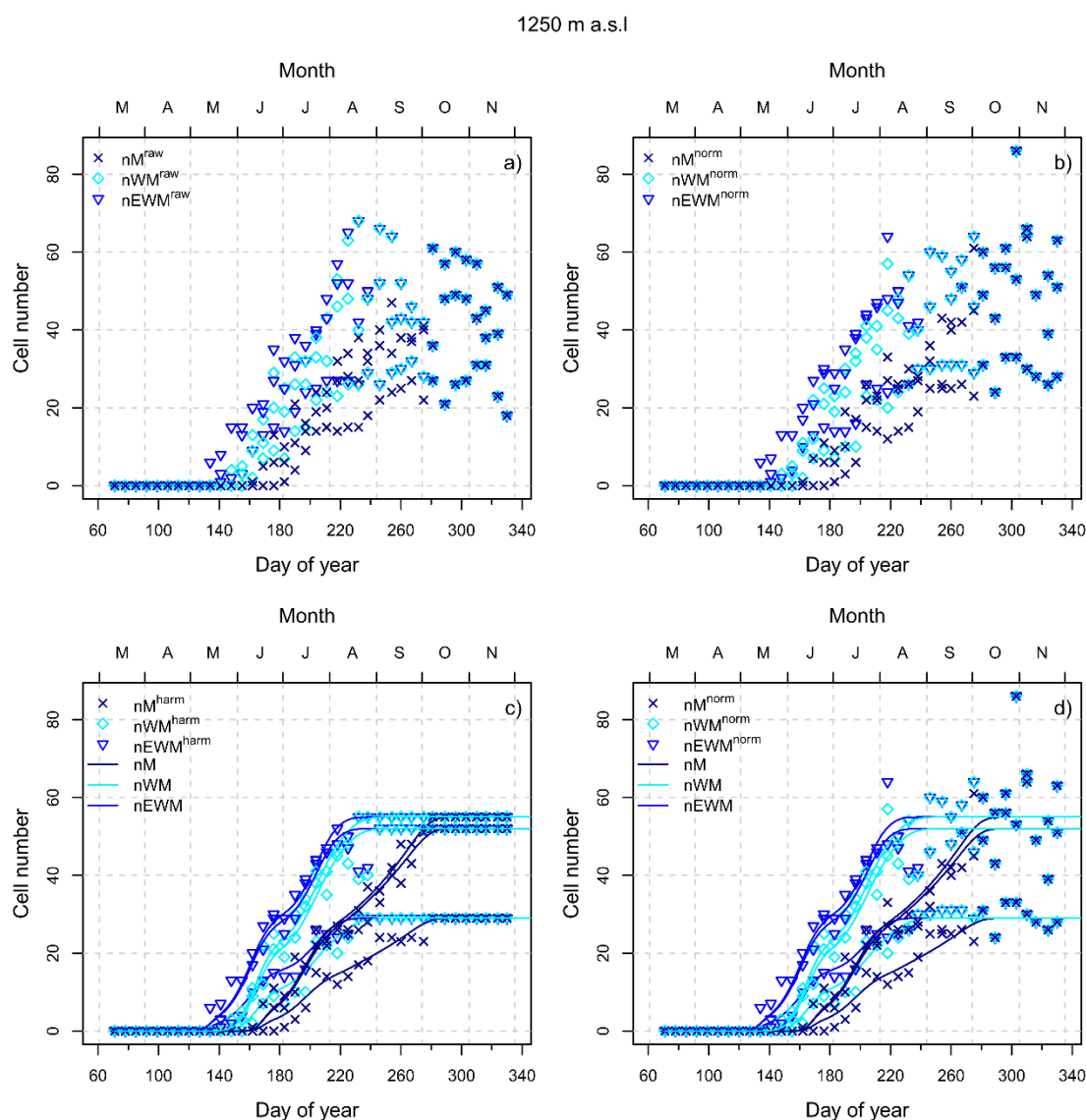
Figure S6. 1250 m a.s.l. elevation site: (**a**) Raw data of weekly counts of mature cells (nM^{raw}), cells with secondary cell walls (nWM^{raw}) and total number of xylem cells ($nEWM^{raw}$), (**b**) Normalized data of mature cells (nM^{raw}), cells with secondary cell walls (nWM^{raw}) and total number of xylem cells ($nEWM^{raw}$), (**c-d**) Tree individual predictions of the definite daily number of mature cells (nM), cells with secondary walls (nWM) and total number of xylem cells ($nEWM$) based on shape constrained additive mixed models in comparison to the harmonized (nM^{harm}, nWM^{harm}, $nEWM^{harm}$) and normalized data (nM^{norm}, nWM^{norm}, $nEWM^{norm}$). One data point reflects for each day of year one of three sampled trees.
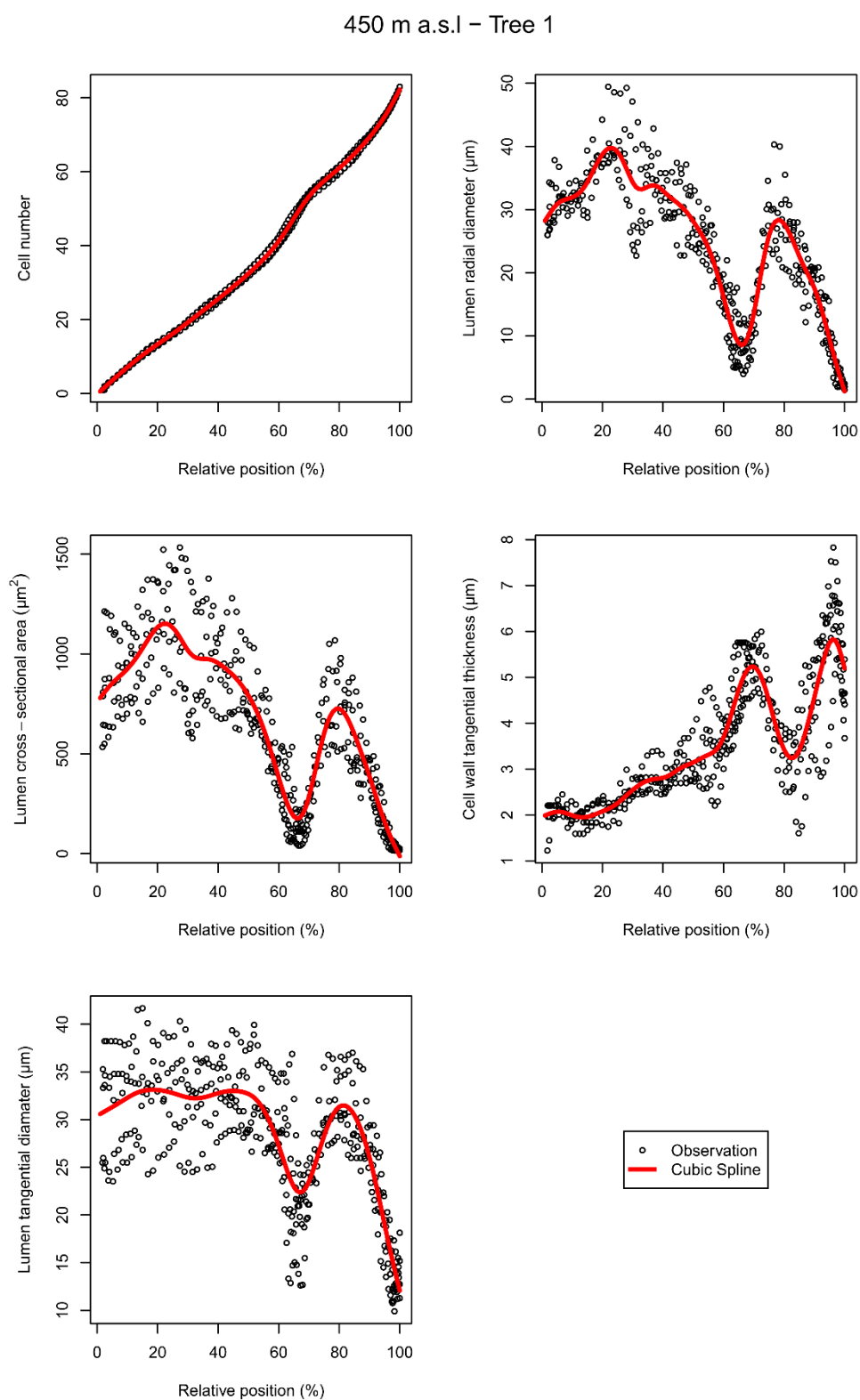
450 m a.s.l − Tree 1

Figure S7. Fits of cubic smoothing splines to the raw data of wood anatomical variables based on 5 analyzed tracheid files of tree number 1 of the 450 m a.s.l. elevation site.
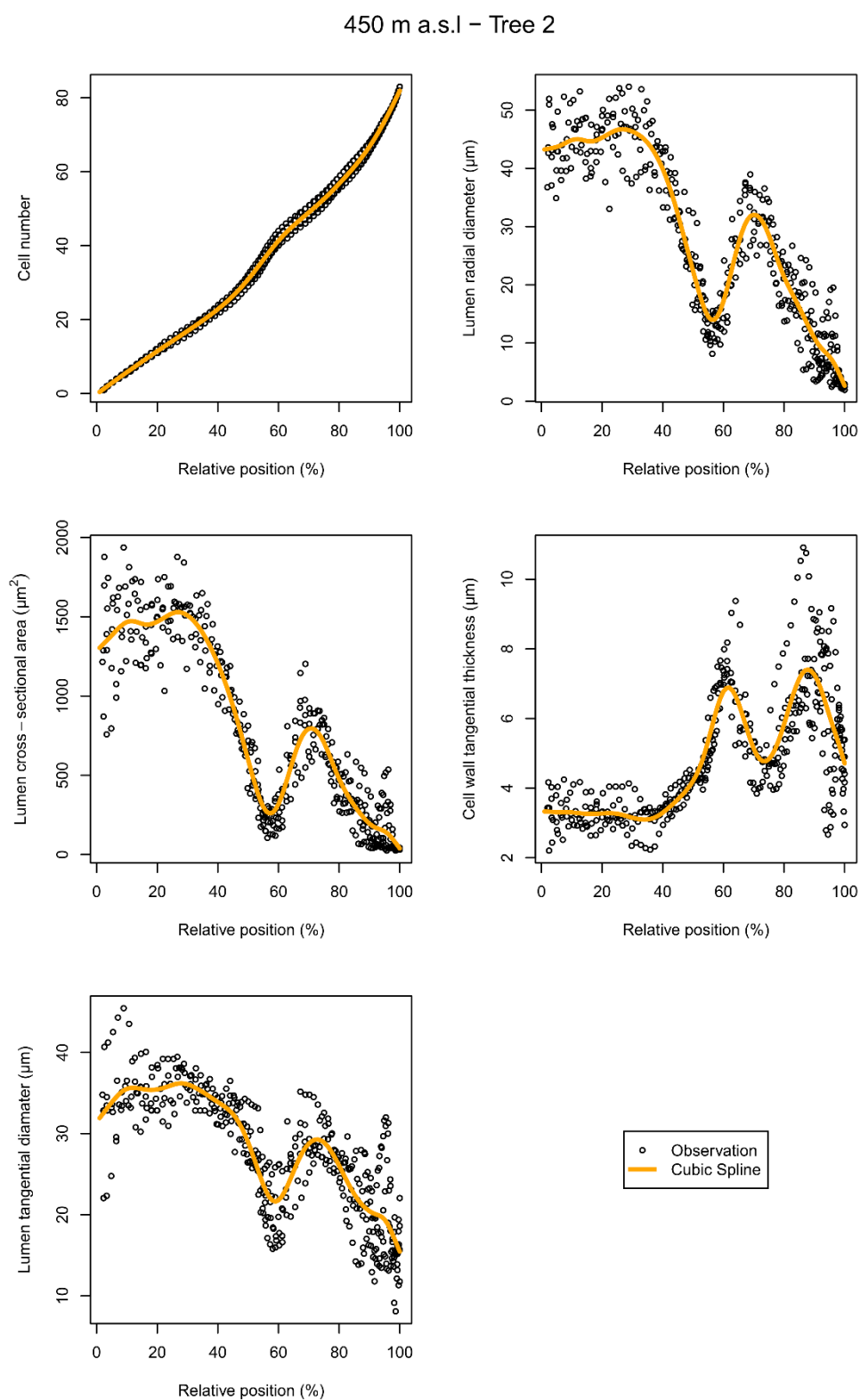
450 m a.s.l − Tree 2

Figure S8. Fits of cubic smoothing splines to the raw data of wood anatomical variables based on 5 analyzed tracheid files of tree number 2 of the 450 m a.s.l. elevation site.
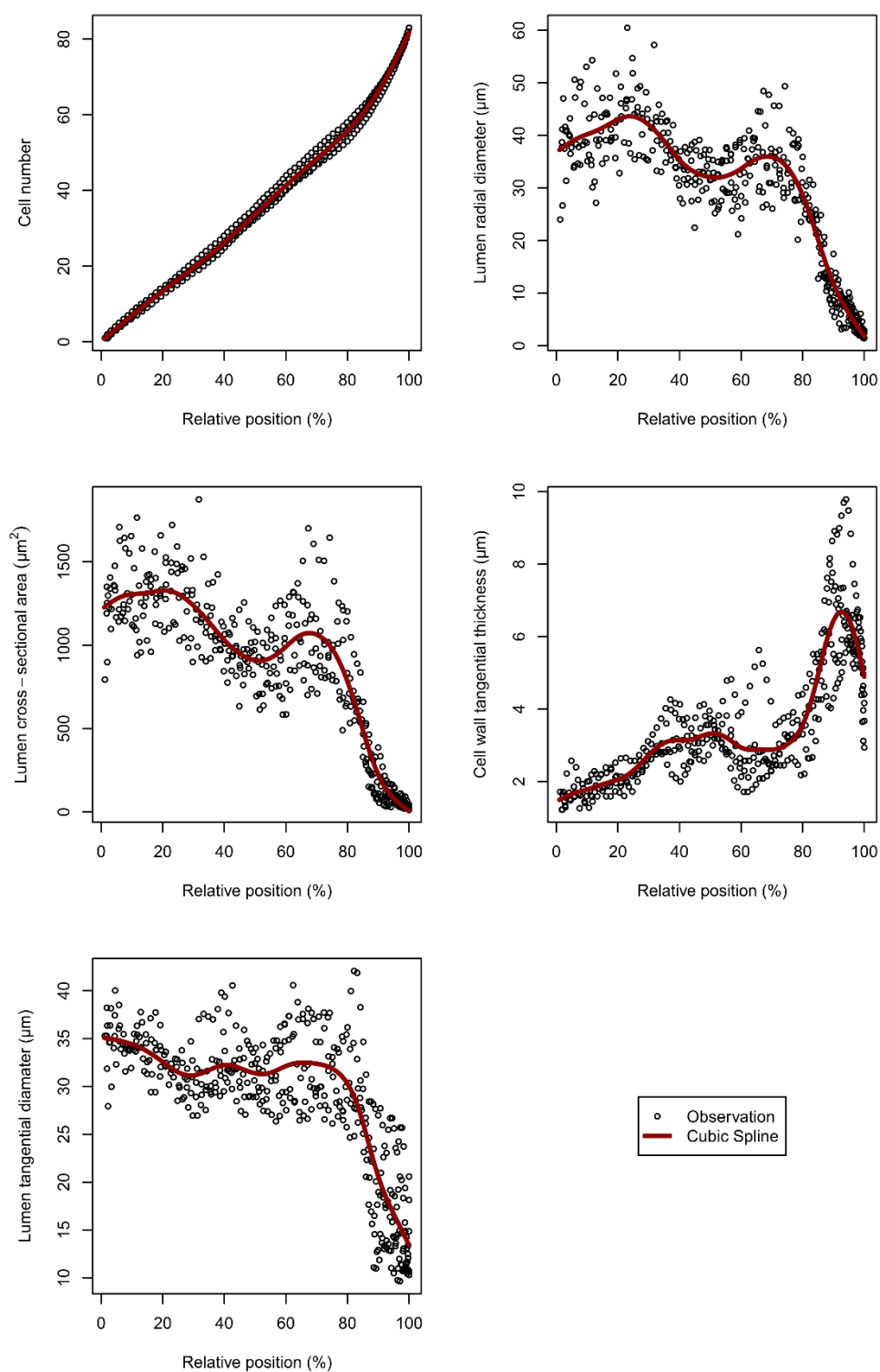
450 m a.s.l − Tree 3

Figure S9. Fits of cubic smoothing splines to the raw data of wood anatomical variables based on 5 analyzed tracheid files of tree number 3 of the 450 m a.s.l. elevation site.
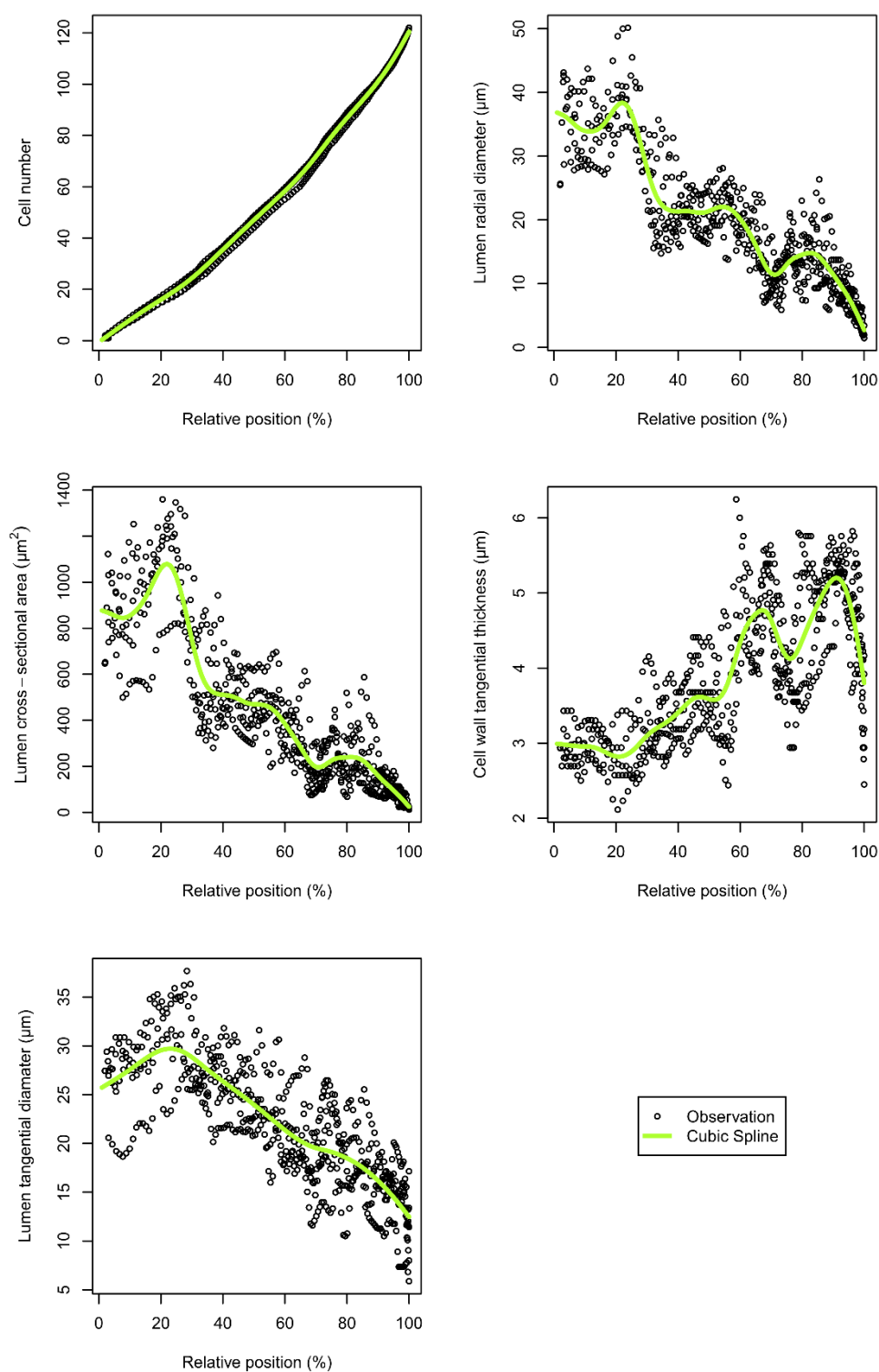
750 m a.s.l − Tree 1

Figure S10. Fits of cubic smoothing splines to the raw data of wood anatomical variables based on 5 analyzed tracheid files of tree number 1 of the 750 m a.s.l. elevation site.
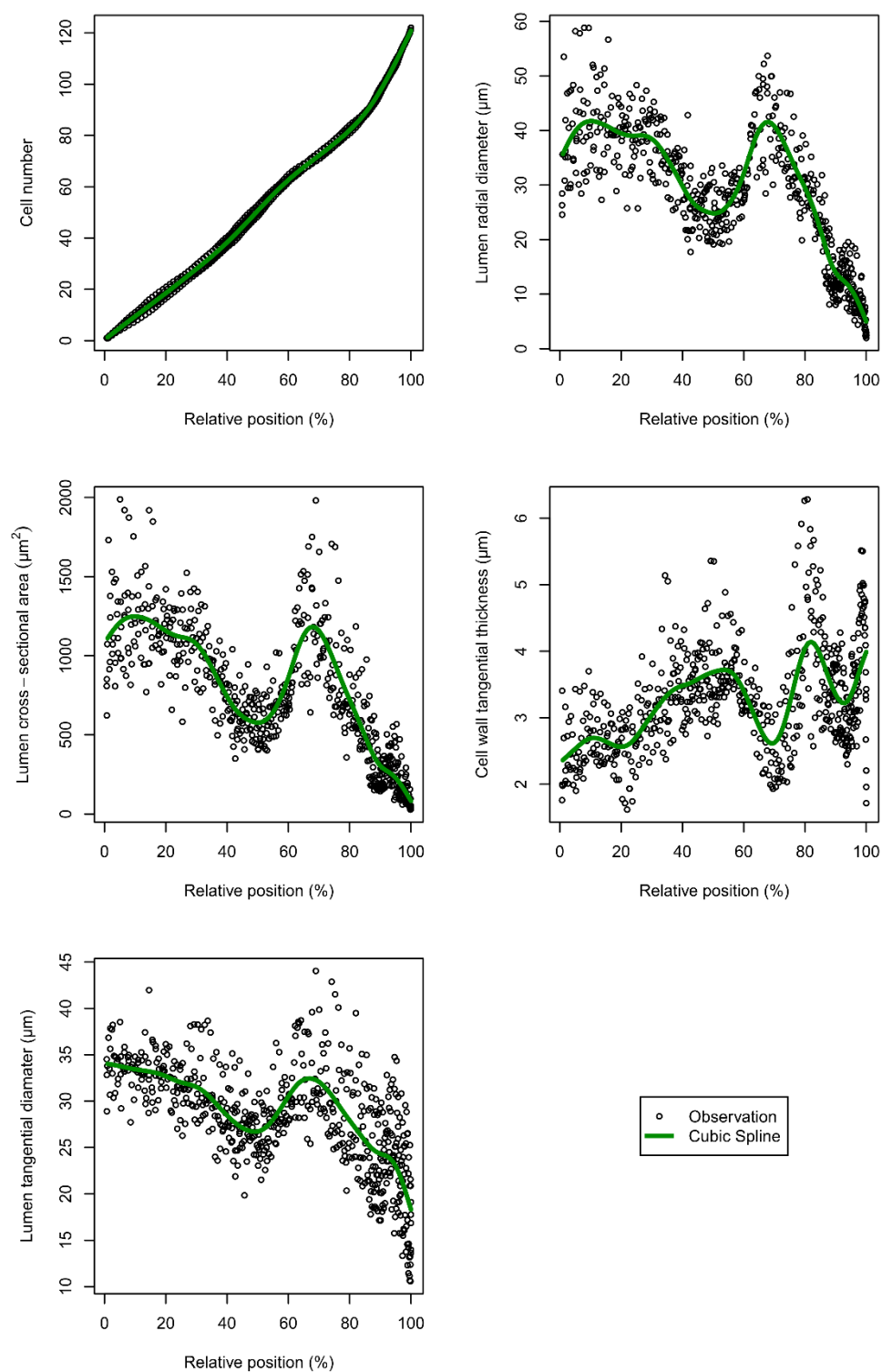
750 m a.s.l − Tree 2

Figure S11. Fits of cubic smoothing splines to the raw data of wood anatomical variables based on 5 analyzed tracheid files of tree number 2 of the 750 m a.s.l. elevation site.

750 m a.s.l − Tree 3

Figure S12. Fits of cubic smoothing splines to the raw data of wood anatomical variables based on 5 analyzed tracheid files of tree number 3 of the 750 m a.s.l. elevation site.
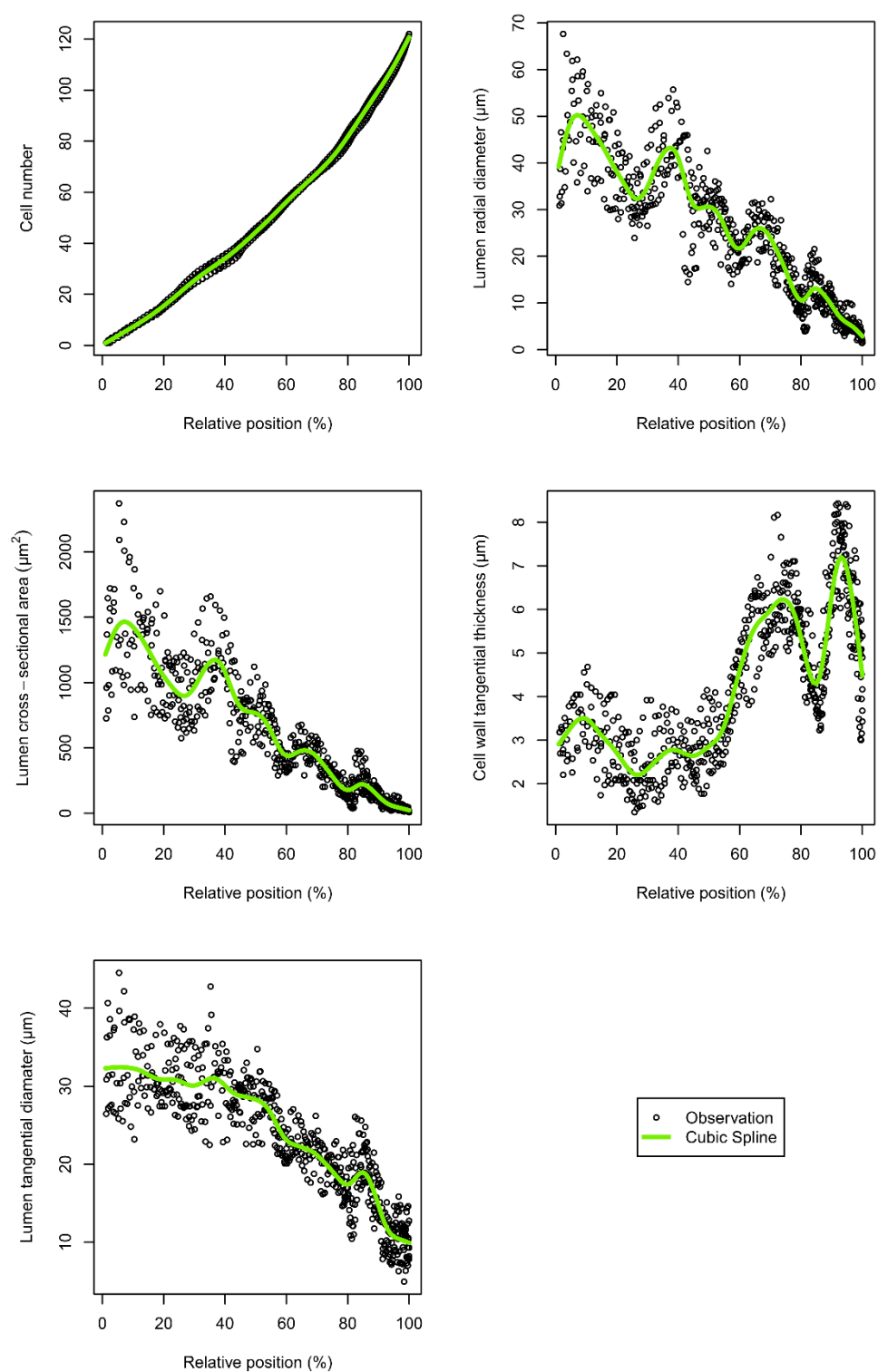
1250 m a.s.l − Tree 1

Figure S13. Fits of cubic smoothing splines to the raw data of wood anatomical variables based on 5 analyzed tracheid files of tree number 1 of the 1250 m a.s.l. elevation site.

Figure S14. Fits of cubic smoothing splines to the raw data of wood anatomical variables based on 5 analyzed tracheid files of tree number 2 of the 1250 m a.s.l. elevation site.

1250 m a.s.l − Tree 3

Figure S15. Fits of cubic smoothing splines to the raw data of wood anatomical variables based on 5 analyzed tracheid files of tree number 3 of the 1250 m a.s.l. elevation site.
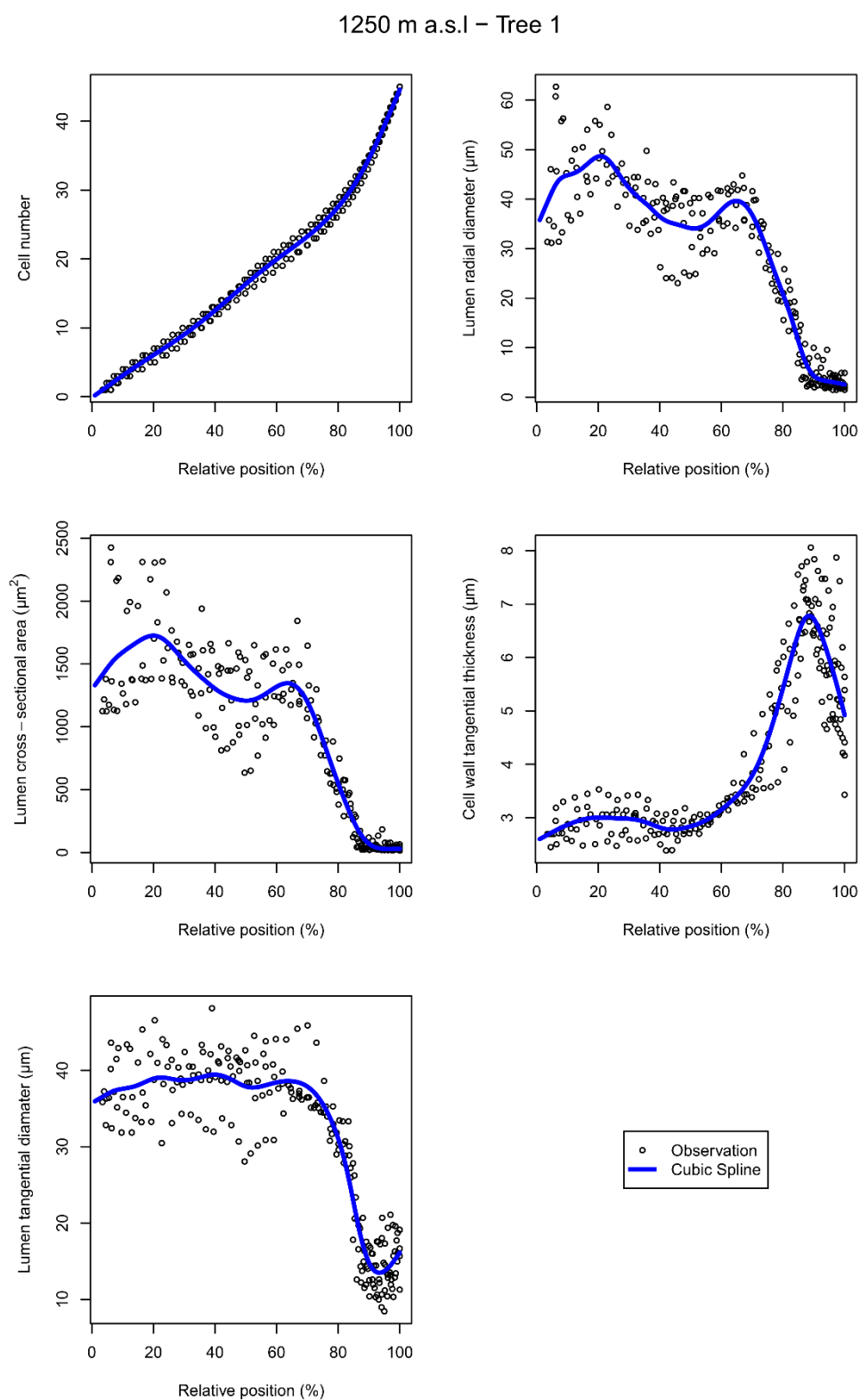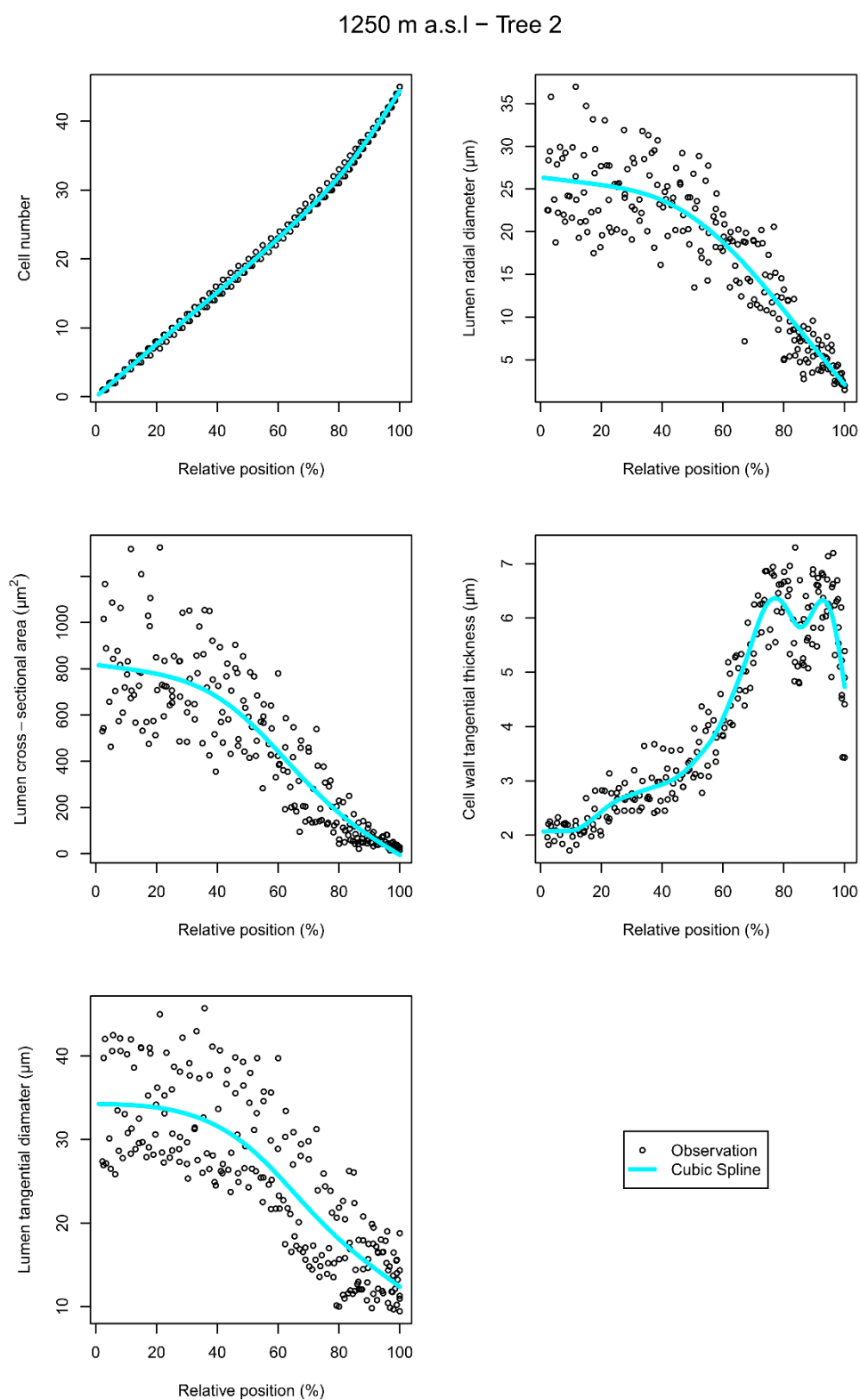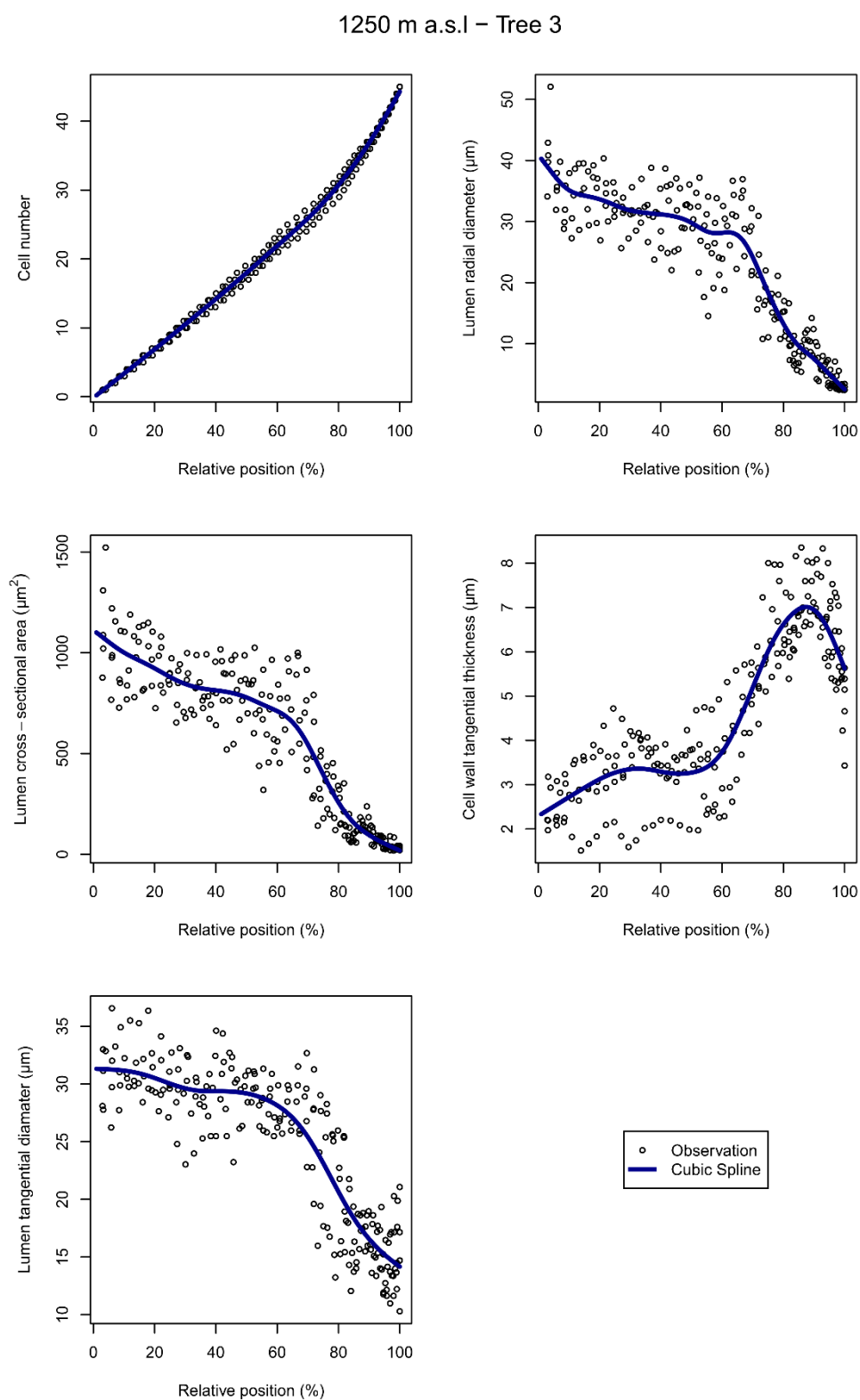
Figure S16. (left) Non-aligned profiles of cell lumen radial diameter (*LRD*) scaled to relative position (relative spatial annotation) for the 450 m, 750 m and 1250 m a.s.l. elevation sites, respectively. (**center**) MICA alignment of the *LRD* profiles in relative spatial annotation. (**right**) MICA aligned *LRD* profiles converted to temporal annotation representing the average day of cell formation for each corresponding *LRD*.

Table S1. Modeling efficiency of the models fitted to the normalized xylogenesis count data and the wood anatomical raw data. Coefficients were calculated on the tree level and then averaged on the stand level. Xylogenesis data: Number of cambial cells (*nC*), number of enlarging cells (*nE*), number of wall thickening cells (*nW*), number of mature cells (*nM*), number of cells with secondary cell walls (*nWM*) and total number of xylem cells (*nEWM*). Wood anatomical data: Cell number (*CN*), lumen radial diameter (*LRD*), lumen cross-sectional area (*LCA*), cell wall tangential thickness (*WTT*), lumen tangential diameter (*LTD*) [5].

Elevation	nC	nE	nW	nM	nWM	nEWM	CN	LRD	LCA	WTT	LTD
450 m a.s.l.	0.466	0.788	0.857	0.898	0.895	0.888	0.998	0.906	0.873	0.772	0.734
750 m a.s.l.	0.639	0.717	0.746	0.921	0.905	0.893	0.999	0.866	0.836	0.666	0.698
1250 m a.s.l.	0.598	0.826	0.899	0.945	0.938	0.937	0.997	0.889	0.854	0.872	0.802

Table S2. Mean absolute error of the models fitted to the normalized xylogenesis count data and the wood anatomical raw data. Coefficients were calculated on the tree level and then averaged on the stand level. Xylogenesis data: Number of cambial cells (*nC*), number of enlarging cells (*nE*), number of wall thickening cells (*nW*), number of mature cells (*nM*), number of cells with secondary cell walls (*nWM*) and total number of xylem cells (*nEWM*). Wood anatomical data: Cell number (*CN*), lumen radial diameter (LRD), lumen cross-sectional area (*LCA*), cell wall tangential thickness (*WTT*), lumen tangential diameter (*LTD*) [5].

Elevation	nC	nE	nW	nM	nWM	nEWM	CN	LRD	LCA	WTT	LTD
450 m a.s.l.	1.48	0.87	2.08	6.89	8.07	8.25	0.80	3.17	121.73	0.55	3.00
750 m a.s.l.	1.70	1.45	3.19	9.04	10.42	11.28	1.06	3.43	115.59	0.46	2.73
1250 m a.s.l.	1.51	0.67	1.05	2.67	3.15	3.26	0.55	3.11	123.06	0.46	3.28

Table S3. Mean absolute percentage error of the models fitted to the normalized xylogenesis count data and the wood anatomical raw data. Coefficients were calculated on the tree level and then averaged on the stand level. Xylogenesis data: Number of cambial cells (*nC*), number of enlarging cells (*nE*), number of wall thickening cells (*nW*), number of mature cells (*nM*), number of cells with secondary cell walls (*nWM*) and total number of xylem cells (*nEWM*). Wood anatomical data: Cell number (*CN*), lumen radial diameter (*LRD*), lumen cross-sectional area (*LCA*), cell wall tangential thickness (*WTT*), lumen tangential diameter (*LTD*) [5].

Elevation	nC	nE	nW	nM	nWM	nEWM	CN	LRD	LCA	WTT	LTD
450 m a.s.l.	16.04	32.68	23.59	16.82	16.07	15.57	1.90	12.53	17.59	13.42	10.85
750 m a.s.l.	15.62	36.52	31.07	16.91	16.55	16.81	1.72	14.79	20.61	11.96	11.42
1250 m a.s.l.	14.64	34.25	21.01	13.93	12.66	11.97	2.38	14.78	20.93	10.25	12.68

Table S4. List of wood anatomical variables used in this study and their method of acquisition based on [6,7].

Variable	Notation	Unit	Acquisition
Cell lumen radial diameter	*LRD*	μm	Measured
Cell lumen tangential diameter[1]	*LTD*	μm	Measured
Cell lumen cross-sectional area	*LCA*	μm²	Measured
Cell wall tangential thickness	*WTT*	μm	Measured
Cell radial diameter	*CRD*	μm	$CRD = LRD + WTT \times 2$
Cell tangential diameter	*CTD*	μm	$CTD = LTD + WTT \times 2.4$
Cell cross-sectional area	*CCA*	μm²	$CCA = CRD \times CTD$
Cell wall cross-sectional area	*WCA*	μm²	$WCA = CCA - LCA$
Mork's Criterion	*MC*	Unitless	$MC = (WTT \times 4) / LRD$

[1] As the last latewood cells occasionally had cell lumen cross-sectional areas in crescent shape, the linear measurement of cell lumen tangential diameter might underestimate their actual dimension. Therefore, if the quotient of cell lumen cross-sectional area and cell lumen radial diameter was higher than the actual measurement of cell lumen tangential diameter, the value of the quotient was considered more representative and appropriate.
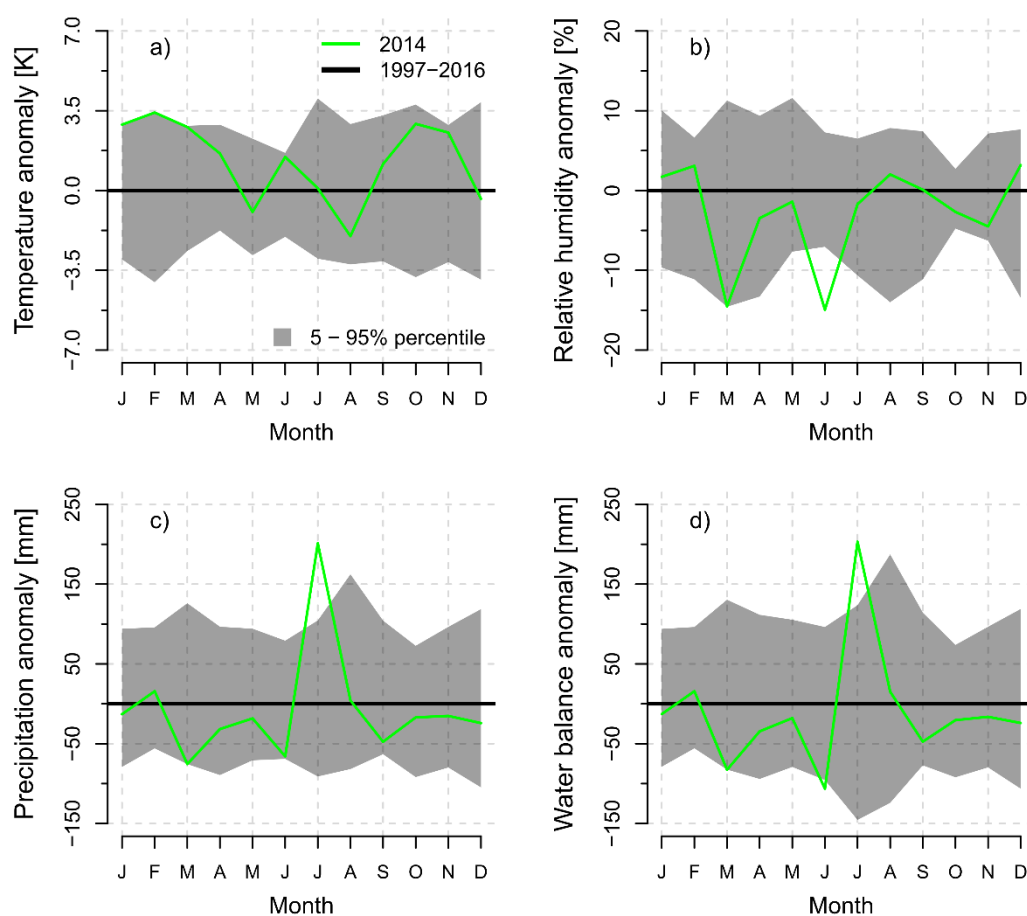
Figure S17. Monthly anomalies of (**a**) air temperature, (**b**) relative humidity, (**c**) monthly precipitation sum and (**d**) climatic water balance (modeled according to Haude [8]) for the 750 m a.s.l. site during the year 2014 as a deviation from the 20-year baseline climate period 1997-2016 (bold horizontal zero line). Shaded areas represent for the baseline climate period (1997-2016) the 5th and 95th percentile of the annual deviations of the 20-year mean values.
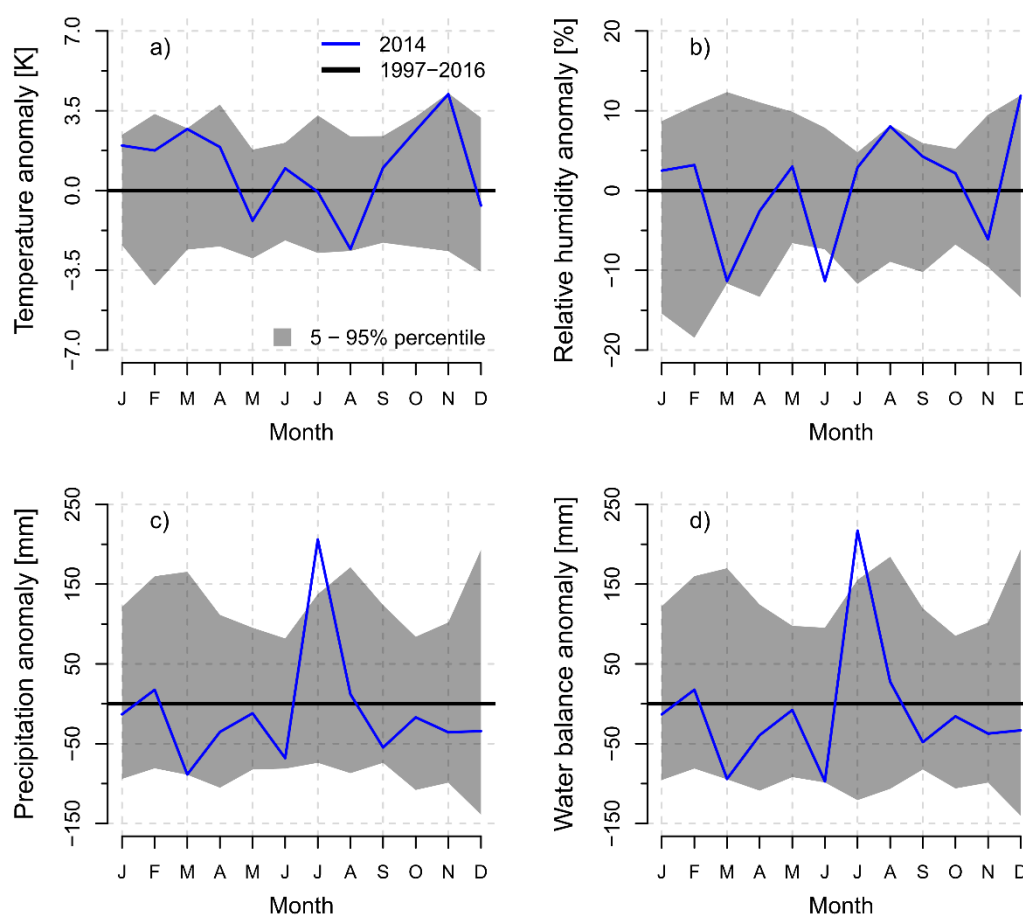
Figure S18. Monthly anomalies of (**a**) air temperature, (**b**) relative humidity, (**c**) monthly precipitation sum and (**d**) climatic water balance (modeled according to Haude [8]) for the 1250 m a.s.l. site during the year 2014 as a deviation from the 20-year baseline climate period 1997-2016 (bold horizontal zero line). Shaded areas represent for the baseline climate period (1997-2016) the 5th and 95th percentile of the annual deviations of the 20-year mean values.

References

1. Rossi, S.; Deslauriers, A.; Morin, H. Application of the Gompertz equation for the study of xylem cell development. *Dendrochronologia* **2003**, *21*, 33–39.

2. Deslauriers, A.; Rossi, S.; Liang, E. Collecting and Processing Wood Microcores for Monitoring Xylogenesis. In *Plant Microtechniques and Protocols,* 1st ed. 2015; Yeung, E.C.T., Stasolla, C., Sumner, M.J., Huang, B.Q., Eds.; Springer: Cham, 2015; pp 417–429, ISBN 978-3-319-19944-3.

3. Wood, S. *Generalized Additive Models*. *An Introduction with R;* CRC Press: Hoboken, 2006, ISBN 9781420010404.

4. Pya, N.; Wood, S.N. Shape constrained additive models. *Stat. Comput.* **2015**, *25*, 543–559, doi:10.1007/s11222-013-9448-7.

5. Mayer, D.G.; Butler, D.G. Statistical validation. *Ecol. Model.* **1993**, *68*, 21–32, doi:10.1016/0304-3800(93)90105-2.

6. Cuny, H.E.; Fonti, P.; Rathgeber, C.B.K.; von Arx, G.; Peters, R.L.; Frank, D.C. Couplings in cell differentiation kinetics mitigate air temperature influence on conifer wood anatomy. *Plant Cell Environ.* **2019**, *42*, 1222–1232, doi:10.1111/pce.13464.

7. Cuny, H.E.; Rathgeber, C.B.K.; Frank, D.C.; Fonti, P.; Fournier, M. Kinetics of tracheid development explain conifer tree-ring structure. *New Phytol.* **2014**, *203*, 1231–1241, doi:10.1111/nph.12871.

8. Haude, W. *Zur Bestimmung der Verdunstung auf möglichst einfache Weise*; Dt. Wetterdienst: Bad Kissingen, 1955.